LAWRENCE
LIVERMORE
NATIONAL
LABORATORY

UCRL-JRNL-229868

# Isochoric Implosions for Fast Ignition

D. S. Clark, M. Tabak

April 12, 2007

Nuclear Fusion

# Isochoric implosions for fast ignition

**D. S. Clark and M. Tabak**

Lawrence Livermore National Laboratory, University of California, Livermore, California 94550

E-mail: clark90@llnl.gov

**Abstract.** Various gain models have shown the potentially great advantages of Fast Ignition (FI) Inertial Confinement Fusion (ICF) over its conventional hot spot ignition counterpart [*e.g.*, S. Atzeni, Phys. Plasmas **6**, 3316 (1999); M. Tabak et al., Fusion Sci. & Technology **49**, 254 (2006)]. These gain models, however, all assume nearly uniform-density fuel assemblies. In contrast, conventional ICF implosions yield hollowed fuel assemblies with a high-density shell of fuel surrounding a low-density, high-pressure hot spot. Hence, to realize fully the advantages of FI, an alternative implosion design must be found which yields nearly isochoric fuel assemblies without substantial hot spots. Here, it is shown that a self-similar spherical implosion of the type originally studied by Guderley [*Luftfahrtforschung* **19**, 302 (1942)] may be employed to yield precisely such quasi-isochoric imploded states. The difficulty remains, however, of accessing these self-similarly imploding configurations from initial conditions representing an actual ICF target, namely a uniform, solid-density shell at rest. Furthermore, these specialized implosions must be realized for practicable drive parameters and at the scales and energies of interest in ICF. A direct-drive implosion scheme is presented which meets all of these requirements and reaches a nearly isochoric assembled density of 300 g/cm$^3$ and areal density of 2.4 g/cm$^2$ using 485 kJ of laser energy.

Submitted to: *Nuclear Fusion*

## 1. Introduction

Fast Ignition (FI) [1] offers an encouraging alternative to the conventional hot spot ignition approach to Inertial Confinement Fusion (ICF) [2]. In the conventional approach, it is the accumulation and stagnation of the hydrodynamic flows at the center of an imploding capsule which produces the extreme temperatures and pressures necessary for fusion ignition. In contrast, for FI, an external energy source (such as the highly energetic electrons produced in intense laser-plasma interactions) is injected into the dense fuel assembly to initiate fusion reactions. Since the fuel assembly and fuel ignition steps are thereby separated in FI, significantly higher gains and more robust targets are projected to be feasible than in the conventional hot spot approach.

While considerable attention has been focused on the beam-plasma interactions integral to FI, *e.g.*, electron beam generation from relativistic laser-plasma interaction,

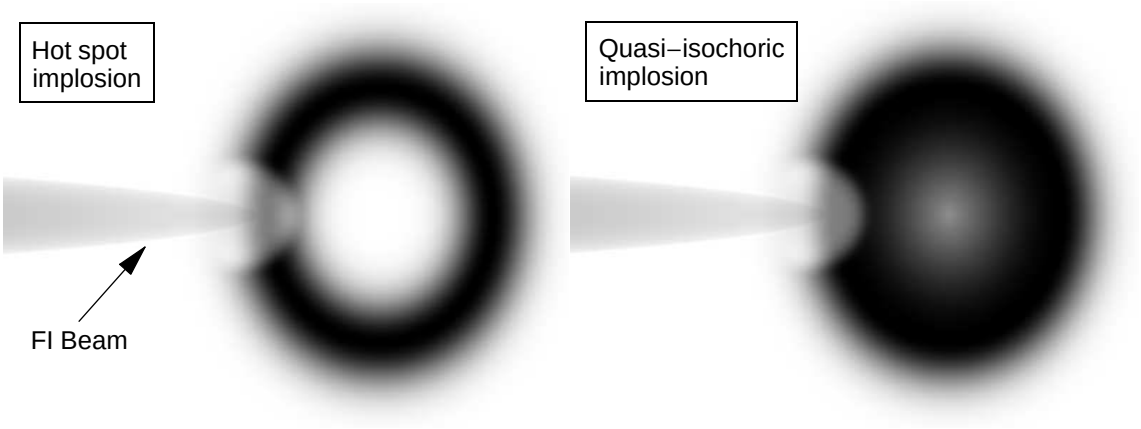


**Figure 1.** Schematic comparison of fast ignition of a typical hot spot fuel assembly and a quasi-isochoric assembly.

the propagation of such beams in dense plasmas, or charged particle stopping in near-Fermi degenerate plasmas, relatively little attention has so far been given to the accompanying hydrodynamics of FI implosions. This omission is especially noteworthy given that, with their externally supplied ignition sources, FI implosions optimize with different imploded fuel configurations than their conventional counterparts. In particular, while the conventional approach is fundamentally dependent on the formation of a robust hot spot to ignite, this central hot spot is in fact a liability in FI. Since ignition occurs effectively from the outside of the fuel assembly in FI, the fusion burn wave in a FI target would propagate predominantly around the edge of a hot spot fuel assembly where the fuel density is high. In a high aspect ratio hot spot implosion, this would amount to nearly two-dimensional burn front propagation. It is evident that if a near-uniform density, or isochoric, fuel assembly could be arranged, the burn wave would propagate much more efficiently through the fuel, namely directly through the center of the implosion in a more three-dimensional manner. Figure 1 schematically contrasts these hot spot and quasi-isochoric fuel assemblies in FI.

Somewhat more quantitatively, it can readily be shown that isochoric implosions achieve higher areal densities (integrated $\rho r$) than conventional hot spot implosions for the same peak density and imploded mass (a rough surrogate for implosions requiring the same hydrodynamic energy investment). Specifically, the areal density of an isochoric implosion is higher than the hot spot implosion of equivalent mass by the aspect ratio of the hot spot to the two-thirds power. This enhancement can amount to a factor of several for typical hot spot implosions. As a consequence, higher burn fractions can be expected in isochoric FI assemblies than in their hot spot counterparts. Furthermore, the gain models which have been proposed for FI target design (and cited to demonstrate its advantages over conventional hot spot ignition) typically assume a near-uniform spherical fuel assembly as a starting point [3, 4]. A challenge, then, in realizing the potential of FI suggested by these gain models, is whether and how such quasi-isochoric implosions can actually be achieved in practice.

Quite broadly in ICF design and theory, a salient role has been played by the class of solutions characterized by self-similarity. As implied by their name, these specialized solutions have the property of remaining always similar to themselves. That is, translations in space or time amount simply to a rescaling of some fundamental solution whose essential shape is invariant. Mathematically, this similarity property has the highly convenient effect of reducing systems of partial differential equations depending on both space and time variables into ordinary differential equations depending on only a single self-similar variable. The Taylor-Sedov blast wave [5, 6] and the self-similar nonlinear heat wave [7] are two particularly prominent examples of self-similarity from quite disparate areas of ICF-related research.

Historically, solutions of this type have been viewed primarily as idealizations of the real flows encountered in applications. For a particular flow of interest, the very strong constraint of self-similarity is unlikely to be satisfied exactly; nevertheless, the flow might be sufficiently close to self-similarity to make such an approximation, and its mathematical simplicity, quite useful. In this light, these exact self-similar solutions have been utilized primarily for extracting generalized scaling laws to describe broad families of implosions [9, 10] or as test problems in validating computer codes.

A peculiarity of these solutions, however, is that a particular sub-family of solutions represents the implosion of a low density spherical shell into a nearly uniform, high density imploded core. Such an implosion is precisely the isochoric assembly sought as a FI target. Noting this property, the objective of this paper is to use these self-similar implosions as a guide in designing a quasi-isochoric FI target. Merely identifying that these self-similar implosions exist and would be advantageous in FI is not the real challenge, however. Given that the necessary starting point of any real implosion is a spherical shell of fuel of essentially uniform density and at rest, an at best degenerately self-similar state, and that a self-similar implosion is necessarily always similar to itself, the real challenge is to develop a means of transforming the required stationary initial state into the desired self-similarly imploding state. This problem can essentially be conceptualized as determining the pressure pulse which, when applied to the outside of a shell of fuel, will bring it into the intended self-similarly imploding state. More importantly, this transformation must be accomplished at the scales and for the drive energies, intensities, etc. of interest in the ICF context. It will be shown that not only are these self-similar implosions accessible in the late phase of a FI implosion but that these implosions may be favored in yielding high areal densities for relatively low laser energies.

As an aside, it should be noted that other schemes have been proposed for achieving quasi-isochoric implosions. Specifically, doping the capsule central void with a high-$Z$ gas, and so radiating away the hot spot energy, has been proposed as a technique for producing quasi-isochoric implosions [11, 12]. While this is certainly a viable alternative scheme, it has, however, yet to be shown in simulations that a genuinely isochoric assembly can be achieved. The penalty of "poisoning" the capsule central region from useful fusion burn is also obvious. Additionally, the introduction of a high-$Z$ gas, such as

xenon, into the center of a cryogenic capsule entails certain technical challenges of its own on account of differing freezing points between the fuel and high-$Z$ gas. In a similar vein, it may also be noted that there exist self-similar implosions which transform uniform density solid spheres into uniform density solid spheres of arbitrarily high density [13]. While this would appear to make for a particularly simple FI target design, this scheme requires peak drive pressures comparable to the stagnation pressure. Such pressures are untenably high for the densities of interest. Hence, only shell-based self-similar implosions are considered here. Finally, multi-shock, low adiabat ICF implosions have also be proposed to assemble FI targets [8]. These are essentially variations of the conventional ICF implosion scheme optimized to produce minimal hot spot volumes. The design presented here is fundamentally distinguished from these designs in that they theoretically can access assemblies with zero hot spot volume.

The remainder of this paper is organized as follows. The following section reviews the basic theory of self-similar spherical implosions as laid out in the work of Guderley and many others. That a subset of these self-similar implosions yields a quasi-isochoric core after stagnation is noted. Section 3 then addresses the central challenge of accessing such specialized, self-similar implosions from the practical initial condition of a stationary spherical shell. A simple and intuitive procedure is described for achieving this. Section 4 then renders this idealized implosion in the form of a one-dimensional (1-D) ICF target design that fits within the parameter space of realistic laser powers, shell aspect ratios, etc. Section 5 then concludes.

## 2. Self-similar spherical implosions

Since Guderley's pioneering work on the problem of spherically and cylindrically imploding shock waves [14], considerable study has been dedicated to the field of self-similar gas dynamics, particularly in the context of spherical implosions or explosions. A particularly encyclopedic account of these solutions is given by Lazarus [15], and his notation is adopted here. The essential ingredient in all of these self-similar spherical solutions is the *ansatz*, first made by Guderley, that the radial and temporal dependence of the spherical flow enters only through the single self-similar variable $x \doteq t/r^{\lambda}$. With this *ansatz*, comes the necessary decomposition of the dimensional flow variables, radial velocity, sound speed, and density, respectively, according to

$$u(r,t) = -(r/\lambda t)V(x) \tag{1a}$$

$$c(r,t) = \quad (r/\lambda t)C(x) \tag{1b}$$

$$\rho(r,t) = \quad r^{\kappa}R(x) \tag{1c}$$

Here, $\lambda$ and $\kappa$ are numerical parameters and the dimensionless reduced functions $V(x)$, $C(x)$, and $R(x)$ are to be determined. Substituting these expressions into the 1-D spherical Euler equations for adiabatic compressible gas flow reduces that system of three coupled nonlinear partial differential equations to two nonlinear ordinary differential

equations and one perfect integral:

$$\frac{dC}{dV} = \frac{F[V,C(V)]}{G[V,C(V)]} \tag{2a}$$

$$\frac{d\ln x}{dV} = \frac{D[V,C(V)]}{G[V,C(V)]} \tag{2b}$$

$$\text{const.} = \left(\frac{C}{x}\right)^2 R^{1-\gamma}\left[(1+V)R\right]^{[\kappa(\gamma-1)+2(\lambda-1)]/(\kappa+3)} . \tag{2c}$$

$F(V,C)$, $G(V,C)$, and $D(V,C)$ are algebraic functions of their arguments, and $c^2 \doteq \gamma p/\rho$. An ideal gas equation of state is assumed with $\gamma$ the usual ratio of specific heats.

The technique for solving (2), and hence the 1-D Euler equations, is to integrate $(2a)$ for the function $C(V)$ (numerically if necessary), and with that solution then integrate $(2b)$ for $x(V)$. The latter function may then be inverted to determine $V(x)$ and from that $C(x) = C[V(x)]$. The reduced density as a function of the self-similar variable $R(x)$ is then know from the integral $(2c)$. With all three reduced variables determined as functions of $x$, (2) and the definition $x \doteq t/r^\lambda$ then give the solution of Euler's equations in $r$ and $t$. What remains to constrain the fundamental solution $C(V)$ is that the physical solutions $u(r,t)$, $c(r,t)$, and $\rho(r,t)$ satisfy the boundary conditions of the problem at hand. For the implosion of a hollow shell, these conditions are that the pressure (and hence sound speed) and the density of the fluid go to zero at the shell inner edge and that the velocity of the flow be finite at the inner edge and go to zero at $r = \infty$. In the $V - C$ plane in which the solution of $(2a)$ is sought, this means that the solution curve must connect the points $(V,C) = (-1,0)$ and $(0,0)$, corresponding to the shell inner edge and $r = \infty$, respectively. Note that this choice of boundary points sets the velocity scale of the problem to be the velocity at the shell inner edge.

The crucial step in the self-similar solution process is the inversion of the function $x(V)$ for $V(x)$. From $(2b)$, this is seen to be possible provided the function $G(V,C)$ remains non-zero. It is the case, however, that $G(V,C)$ is zero all along the line $C = 1 + V$, a line which must be crossed by the solution curve in progressing from $(V,C) = (-1,0)$ to $(0,0)$. The only way in which this line may be crossed and the solution remain single-valued (*i.e.*, physical) in $x$ is to cross at a singular point where $D(V,C)$ is also zero. This is the fundamental constraint on the solution $C(V)$ which determines the allowed values of $\lambda$ and $\kappa$. The spectrum of this nonlinear eigenvalue problem as a function of $\gamma$ has been extensively investigated [15, 16].

The above procedure outlines the self-similar solution of the Euler equations for the in-going phase of the implosion. Remarkably, the out-going or stagnation phase may also be described self-similarly. For the stagnation of the flow, the solution curve of $(2a)$ in the $V - C$ plane may simply be continued through the point $(V,C) = (0,0)$ to positive $V$ (*i.e.*, outward-flowing velocities); however, reaching the proper physical boundary condition again necessitates crossing a line where $G(V,C) = 0$, in this case $C = -1 - V$. Since there are no suitable points where $D(V,C)$ is zero with positive $V$, single-valuedness in the solution of $(2b)$ now requires that this singular line be crossed in

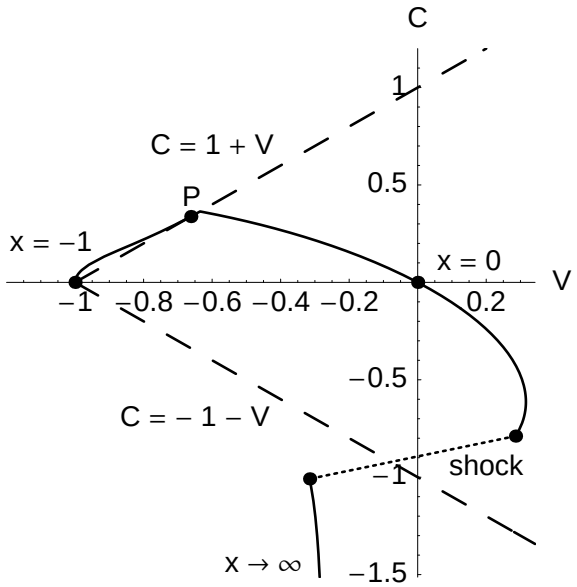


**Figure 2.** A sample self-similar implosion solution in the $V - C$ plane for $\lambda = 1.267$, $\kappa = -0.801$ and for $\gamma = 5/3$.

a discontinuous jump. Physically, this jump simply corresponds to the stagnation shock which reverses the flow velocity from in-going to out-flowing at the stagnation time.

Figure 2 illustrates a sample self-similar solution trajectory, shown as the solid curve, in the $V - C$ plane. The singular lines $C = \pm 1 \pm V$, shown dashed, are crossed at the singular point $P$ and by the shock jump line, shown dotted. As is customary, the self-similar variable has been scaled to be $x = -1$ at the leading edge of the shell. From its definition, $x = 0$ corresponds to the boundary $r = \infty$ or to the entire shell at $t = 0$, and $x \to \infty$ corresponds to $t \to \infty$ for finite $r$ or $r = 0$ for $t > 0$. Hence, the solution in the upper left quadrant of the $V - C$ plane between $x = -1$ and $x = 0$ traces out the profile of the imploding shell. The lower half of the $V - C$ plane, traced from $x = 0$ to $x = \infty$, gives the stagnation phase flow from pre- to post-shock states.

While (2) must in general be integrated numerically, certain asymptotic properties of the solutions can yet be obtained analytically [17]. Specifically, the asymptotic behavior of the physical solutions in the limit $x \to \infty$ is given by:

$$u(r,t) \sim \frac{\mu + \kappa}{\lambda\,\nu\,\gamma}\frac{r}{t} \tag{3a}$$

$$\rho(r,t) \sim r^{q} t^{(q-\kappa)/\lambda} \tag{3b}$$

$$T(r,t) \sim r^{-q} t^{-(\mu+q/\lambda)} \tag{3c}$$

$$p(r,t) \sim r^{0} t^{-(\mu+\kappa/\lambda)} \tag{3d}$$

with

$$q = 2\frac{\kappa(\gamma-1) - 2(\lambda+1)}{2\gamma + \kappa + 2(\lambda+1)} \tag{4a}$$

$$\mu = 2(1 + 1/\lambda) \tag{4b}$$

$$\nu = 2\gamma + \kappa + 2(\gamma+1) \tag{4c}$$

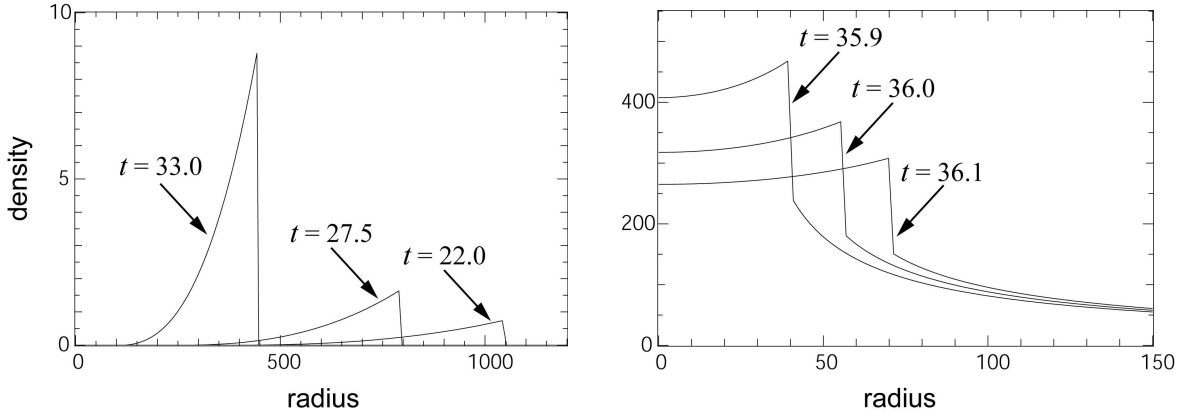


**Figure 3.** Flow profiles during the imploding and stagnating phases of the self-similar isochoric flow given by the solution curve from figure 2. The length and time scales have been normalized to values representative of a typical ICF implosion in the physical units of nanoseconds and microns.

This limit is of particular interest since, from the definition of the self-similar variable $x$, it is evident that these limits give either the late time behavior of the flow, $t \to \infty$, or the flow close to $r = 0$ after void closure. This is precisely the region in space and time that is of greatest interest in target design, *i.e.*, the assembled fuel configuration. Hence, from $(3b)$ the essential prescription for arranging an isochoric self-similar implosion can be read off: the density $\rho(r,t)$ will become asymptotically flat after stagnation if the implosion is driven in such a way that the exponent $q = 0$. Equivalently, for a given choice of $\lambda$, this condition requires setting $\kappa = 2(\lambda+1)/(\gamma-1)$.

Figure 3 plots the density profiles at three selected times from both the implosion and stagnation phases of the self-similar flow corresponding to the solution curve in figure 2. Since the length and time scales may always be normalized arbitrarily, values representative of a typical ICF implosion in the physical units of nanoseconds and microns have been used. The density scale has been normalized to unity at $t = 24.0$. For this solution, the adjustable parameters $\lambda$ and $\kappa$ have been set to 1.267 and $-0.801$, respectively, so that $q = 0$ for $\gamma = 5/3$. The implosion of the initially low density shell into a high-density, quasi-isochoric assembly is clearly evident with a central density of approximately 300 in these units. Theoretically at least, a zero hot spot volume is achieved.

In addition to indicating that the imploded core is quasi-isochoric when $q = 0$, (3) also indicate that the flow is completely isentropic in this case, *i.e.*, the adiabat $p/\rho^\gamma$ is constant not only temporally, since the flow is assumed adiabatic, but also spatially through the shell. In fact, this isentropy is not merely true asymptotically but holds in general aside from the location of the stagnation shock. Isentropy may in effect be taken as the distinguishing characteristic of self-similar flows with $q = 0$: for $q > 0$, the adiabat increases toward the inner edge of the shell and ultimately leads to the formation of a hot spot; for $q = 0$, the adiabat is flat throughout the shell and no hot spot forms; and for $q < 0$, the adiabat decreases towards the inner edge of the shell. As

emphasized by [17], the first, non-isentropic case is a useful model of conventional hot spot implosions. Similarly, the third, non-isentropic case could pertain to implosions driven by the decaying shocks launched by picket-type pulses. Achieving the second, totally isentropic case is the objective here.

The physical reason for the formation of an isochoric assembly is also made clear by considering these adiabats. Since the flow stagnates in a nearly isobaric state independent of $q$ (see $(3d)$), if the flow is arranged also to be isentropic at stagnation, then its final state must perforce be isochoric as well. Dynamically, when $q = 0$, the self-similar inflow of material meeting the stagnation shock is configured precisely such that, even though the shock should weaken as it expands radially, the radially decreasing density which it traverses acts to strengthen the shock and exactly compensate its weakening from expansion. Since the shock is then maintained at a constant strength as it propagates outward, the adiabat and pressure, and therefore also the density, are left with nearly constant values behind it.

Perfectly isentropic implosion solutions of this type are, in fact, well-known from a context very different from ICF: the isentropic collapse of cavitation bubbles in an infinite liquid. This problem was one of the first in fluid mechanics to be addressed self-similarly in the classic solution by Rayleigh [18] and later along the lines of Guderley's method by Hunter [19]. In this case, however, the problem was merely to determine the time asymptotic dynamics of bubble collapse assuming the flow to be isentropic. That the isentropic flow after stagnation is also isochoric was an unremarked side effect. In the context of FI implosion designs, these roles are now reversed, and it is an isochoric assembled state which is being sought by driving the implosion isentropically.

As already noted, the existence of self-similar implosion solutions of the type shown in figure 3 in effect does not solve but only shifts the problem of designing an isochoric implosion. While these solutions demonstrate that such isochoric assemblies are in principle possible, there remains the problem of initiating such implosions. In practice, an implosion must, of course, begin from a shell of uniform density fuel at rest. As illustrated in figure 3, the density distributions during the imploding phase of these flows are far from uniform in addition to being never at rest. The task, then, is to determine a means of transforming the necessarily uniform initial shell into one of these self-similarly imploding shells. The fact that the flow must be arranged to implode with a uniform adiabat also augurs that considerable care will be required in designing the implosion so as not to disrupt the shell adiabat. Furthermore, this transformation must be accomplished recognizing the non-ideal equation of state (EOS) for a real material (not the $\gamma = 5/3$ used in calculating figure 3), the finite thermal conductivity of that material, and the reality of a laser or x-ray drive. The remainder of this paper develops a method for solving this problem in order to realize the isochoric stagnated state pictured in figure 3.

Before proceeding to the design of an isochoric target implosion, it is worth noting a remaining general property of these self-similar solutions. Within the field of self-similar gas dynamics, considerable importance has been attached to the notion that

self-similar solutions are not merely mathematically convenient solutions to the gas dynamic equations but in fact represent uniquely stable solutions in the space of all possible solutions. More importantly, these solutions are broadly regarded as attractor solutions in the space of all solutions. That is, other solutions, beginning from some general non-self-similar initial conditions, are expected to tend towards self-similarity asymptotically in space and time. While the attracting nature of these solutions has been much discussed under the rubric of intermediate asymptotics [20, 21], the proof of this property regrettably remains incomplete. The problem in planar gas flow was addressed by [22, 23], while, for the spherical case, a linear analysis has been made of the stability of solutions in the $V - C$ plane [24]. Some progress in this arena was also made by the simulation work of [25].

Though a rigorous proof that self-similar solutions do behave as attractors has yet to be given, the concept does offer encouragement to the task of arranging a self-similar isochoric implosion. It is a tautology that self-similar flows always remain similar to themselves. A direct consequence, however, is that it would be impossible to match exactly the flow profiles of a self-similar flow to the profiles of the non-self-similar flow that must result from any practical (non-self-similar) initial state. On the other hand, if it is sufficient merely to approximate a self-similar state at some point during the implosion and the flow afterward will then attract asymptotically toward self-similarity, the feasibility of realizing a self-similar isochoric state becomes more plausible. Indeed, the original analysis of isentropic bubble collapse assumed self-similarity to apply only infinitesimally close to the bubble inner edge and at times infinitesimally close to the time of total collapse. The vast bulk of the flow was assumed not to be self-similar but also not to break the similarity of the flow close to the collapse point. In a similar fashion, this attraction to self-similarity at late times and over an infinitesimal volume will be exploited in the design to follow.

## 3. Initiating self-similar implosions from a stationary uniform shell

Any practical ICF implosion begins from an initial shock. This shock is an inevitable consequence of the discontinuous switching-on of the laser or other driving beam. Representative of ICF implosions, an initial shock of 1.0 Mbar impinging on a shell of DT ice at density $0.25\,\mathrm{g/cm^3}$ is assumed here. Following such a shock, the DT fuel density is $\sim 1.0\,\mathrm{g/cm^3}$, the flow velocity is $\sim 10^6\,\mathrm{cm/s}$, and the plasma, though not perfectly ionized, behaves in some respect as a $\gamma = 5/3$ gas as assumed in the self-similar solution. For a typically high aspect ratio initial shell, a near uniform adiabat is also established throughout the shell.

In typical ICF implosions, a train of three to four shocks is launched into the fuel with each timed so as to overtake the others nearly simultaneous with their breakout from the shell inner edge [2]. While this scheme, in principle, leaves the entire shell on the same adiabat and can raise the fuel density to $\sim 10.0\,\mathrm{g/cm^3}$ or more, it requires extremely precise timing of the pressure pulse. Any mistiming in the launching of these

shocks, causing one shock to overtake another prematurely or one shock to break out ahead of the others, leads to substantial increases in the adiabat at the shell inner edge. Such increases in the adiabat, though undesirable, are not catastrophic for an implosion which is designed ultimately to form a hot spot. If a hot spot is to be avoided, however, as for an isochoric implosion, such mistimings can be ill afforded. Hence, while a multi-shock scheme is theoretically compatible with a totally isentropic implosion, the design below is constrained to a single initial shock. This constraint proves not unduly to limit the final imploded density but does significantly enhance the robustness of the design.

Following the break out of the initial shock, a rarefaction wave travels back into the shell from the inner edge at the post-shock sound speed. Once this rarefaction reaches the outer edge of the shell, isentropic flow profiles in density, pressure, and velocity will have been established throughout the shell. These profiles are, however, far from the self-similar profiles pictured in figure 3 and can hardly be expected to attract to the isochoric imploded state also pictured in figure 3. A scheme for accessing the self-similar regime other than this simple shock and rarefaction is evidently required.

Fortunately, in addition to discrete shock waves and simple rarefactions, the flow may also be driven isentropically by any of a continuous family of isentropic compression waves [26]. These are typically manifest as monotonic and synchronized ramps in the density, pressure, flow velocity, etc. but without corresponding perturbations of the adiabat. Since they are by definition isentropic, they also advance along the characteristics of the flow. In particular, for an isentropic compression following a shock, the leading edge of the compression wave travels along the straight characteristic of the uniform, shocked flow ahead of it. Such a compression wave may then easily be timed to breakout from the inner shell edge simultaneous with the preceding shock. (Note that, as with a multi-shock drive, any overtaking of the shock by the compression wave results in a non-isentropic strengthening of the shock and perturbation of the shell adiabat. However, unlike the shock case, delayed breakout of the compression wave relative to the shock does not lead to non-isentropic flow.) Following the shock and compression wave breakout, the subsequent rarefaction interacts with a non-uniform but still isentropic flow and the subsequent flow profiles adjust accordingly. Intuitively, this arrangement of a shock followed by a synchronized isentropic compression wave and the subsequent rarefaction can then be seen as a sequence of levers with which to shape the flow profiles toward self-similarity without perturbing the adiabat.

The question then is which member of the family of isentropic compression waves will, when coupled with the preceding shock and subsequent rarefaction, adjust the flow profiles to the desired self-similar isentropic state. Regrettably, it does not appear possible from first principles to choose a compression wave profile which will lead directly to a self-similarly imploding configuration such as pictured in figure 3. The primary complication here is the substantial spherical convergence of the flow during the phase in which it must adjust toward self-similarity. The classical techniques of the Riemann invariants and characteristics for isentropic gas flow may be employed to match a wide range of flow profiles relevant to self-similar flows but only in the

planar approximation. The non-negligible convergence of the shell as its profiles are being shaped, unfortunately, renders such techniques inapplicable. Some other shaping approach is required in the presence of this significant convergence.

A technique for choosing the appropriate compression wave profile or, equivalently, pressure history may be intuited by viewing this flow from a different perspective, a perspective which exploits the attracting nature of self-similar flows. Recalling that, in the original self-similar solution of the collapsing cavity problem, self-similarity was assumed to apply only to the very inner-most edge of the cavity and only at times close to the time of total collapse, the self-similarly imploding shell in an FI implosion may be imagined merely as the leading edge of a larger non-self-similar imploding flow. While an extended "fictitious" flow, initialized by some chosen isentropic compression wave, may be evolving in some non-self-similar way, the leading edge of this flow, representing the "real" imploding shell, should, according to the principles of intermediate asymptotics, progressively attract toward self-similarity. The desired pressure history to drive the "real" shell to self-similarity, including the effects of convergence, is then simply the pressure history experienced at the boundary between these "real" and "fictitious" flows.

The precise values of the pressure history may be calculated by simply simulating numerically these conceptualized "real" and "fictitious" flows. That is, a shell several times the intended shell thickness is initialized in a simulation with the velocity and pressure profiles appropriate to a "fictitious" wave. (The condition on the initial thickness of this shell is simply that the transit time for the inner edge rarefaction to the simulation boundary exceed the implosion time of the shell leading edge.) As the compression wave isentropically drives the shell inward, the pressure experienced at the physical location of the back of the shell can be recorded and subsequently used to drive the implosion in the "real" shell of the intended thickness. By simply following the simulation results through the time of void closure and stagnation, the entire pressure history needed for such an asymptotically self-similar implosion may simply be read off.

Figure 4 illustrates this division of an imploding flow into "real" and "fictitious" components in six snapshots from a 1-D simulation run with the HYDRA code [27]. The shock and succeeding isentropic compression wave (extracted from the classic Riemann solution for isentropic compression of an ideal gas [26]) are evident in the "fictitious" flow component of the first snapshot. Subsequent snapshots show the instant of shock breakout, the shell rarefaction, and the eventual stagnation of the flow. As is also evident, the compression wave has been timed to overtake the shock simultaneous with the shock breakout. Anticipating the application to ICF, the physical dimension of $1000\,\mu$m has been chosen for the initial radius of the collapsing void, and the initial shell thickness was set to $230\,\mu$m. In place of the ideal gas EOS used above, the physically accurate QEOS model [28] for DT has also been introduced at this point. The non-ideal effect of this realistic EOS as well as the accumulated imperfections of the discretized numerical solution are evident in the distortions in the imploded core. Nonetheless, the stagnated density distribution is quite uniform and comparable to that in figure 3. An extremely small hot spot is apparent in the stagnated flow due to the finite central gas

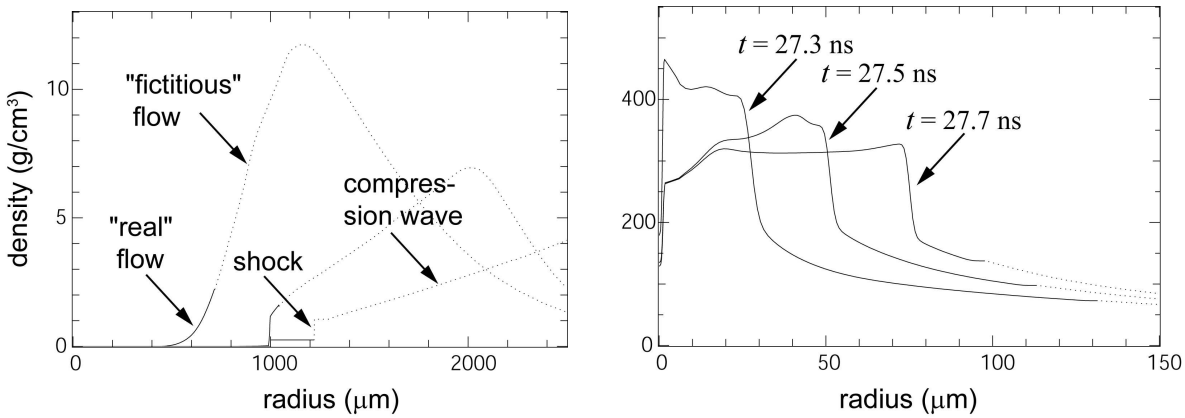


**Figure 4.** Illustration of the "real" and "fictitious" flows used in isentropically approaching self-similarity. The solid line denotes the "real" component of the flow and the dotted line the "fictitious" component.

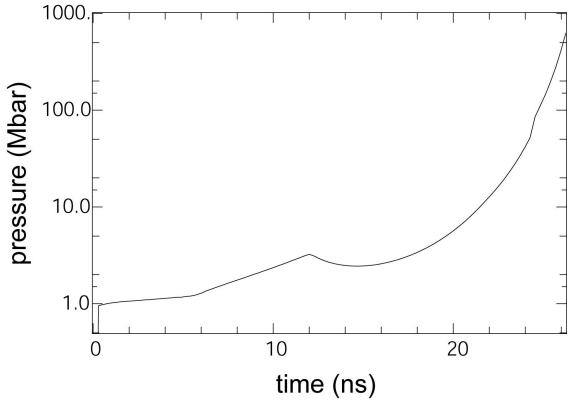


**Figure 5.** Pressure history for initiating and driving a self-similar implosion as recorded from the continued "fictitious" flow pictured in figure 4.

fill of $10^{-6}$ g/cm$^3$ initialized in the simulation; however, from a practical perspective, this hot spot volume may be taken to be essentially zero. Note that the $10^6$cm/s velocity scale established by the 1.0 Mbar shock, coupled with this 1000 $\mu$m spatial scale, has also established a 10 ns time scale.

The resulting pressure history recorded from the Lagrangian trajectory at the back of the "real" shell in figure 4 is shown in figure 5. Visible are the shock, compression wave, rarefaction, and final attraction to self-similarity. Combined with the fuel layer thickness and radius from figure 4, figure 5 represents the essential ingredient needed for a quasi-isochoric target design.

While the results pictured in figure 4 are certainly self-similar in character, the procedure described here does not make use of the underlying self-similar theory in a prescriptive way. This is due to the inevitably non-self-similar character of the flow during the transition period between the initial conditions and the asymptotic state. Such non-self-similar imploding states seem simply not amenable to analytic treatment. In particular, this approach is not *a priori* predictive of what assembled density may be

achieved. Nevertheless, a suite of implosions may easily be simulated with compression waves of increasing strength, and the optimal shape of the "fictitious" wave determined by trial and error. An upper bound is placed on the compression wave strength by the constraint the wave not steepen into a shock prior to the time of void closure. Such shocking of the fuel would clearly disrupt the isentropic character of the flow and produce a hot spot. Empirically, the compression wave shown in figure 4 was found to be the strongest wave allowed which did not lead to premature shocking of the fuel. Outside of this constraint, so long as the flow is initialized in an isentropic state, the subsequent attraction to self-similarity should remain isentropic and lead to the intended isochoric assembly.

In addition to the strength of the compression wave, the initial aspect ratio of the "real" shell also provides a variable with which to adjust the degree of compression in the core. As is well-known from conventional ICF implosions, high aspect ratio shells achieve the most mechanical efficiency and highest compression. However, in the self-similar context, high aspect ratios also place the highest premium on a precise drive history. This is due to the resulting minimal separation between the exterior non-self-similar flow and the interior flow which is attracting toward self-similarity. High aspect ratio implosions are thus most prone to deviating from self-similarity and stagnating in a non-isochoric configuration. A balance must evidently be struck between these competing objectives. The aspect ratio chosen for the implosion in figure 4 represents such a compromise between achieving a robustly isochoric assembly and a mechanical efficient implosion.

## 4. A quasi-isochoric target design

The procedure outlined in the preceding section is sufficient to drive an initially stationary and uniform density shell to an approximately self-similarly imploding state and from there to the isochoric stagnated state desired for FI. From the perspective of ICF target design, the remaining challenge is then to determine what laser pulse (or other driving beam) history and what specific target design is required to deliver this pressure history to the shell of fuel. For simplicity, only a direct drive target design is considered here.

Given the complexity of the physical processes involved in the laser absorption, ablation, and hydrodynamic recoil of the target, the laser pulse shape and specific ablator thickness necessary to deliver the pressure pulse to the fuel layer are best determined simply by numerical trial and error. The eventual target design that was converged on is shown in figure 6 along with the laser pulse history. As in section 3, the target consists of a $1000\,\mu$m central void and a $230\,\mu$m thick DT fuel layer. The central gas fill was again taken to be $10^{-6}\,\mathrm{g/cm^3}$ corresponding to a target temperature of $< 15\,\mathrm{K}$ [29]. To accommodate the laser drive, a $180\,\mu$m thick ablator of CH foam wicked with DT is added. A 12.0% CH atomic concentration was chosen for the ablator so as to prevent radiation pre-heating of the fuel layer which could disrupt the fuel adiabat and timing

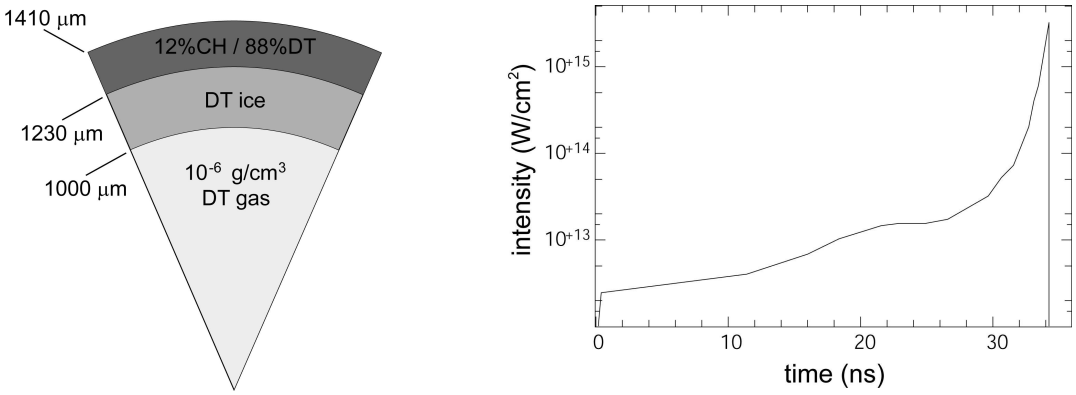


**Figure 6.** Target composition and laser drive for an example quasi-isochoric FI implosion.

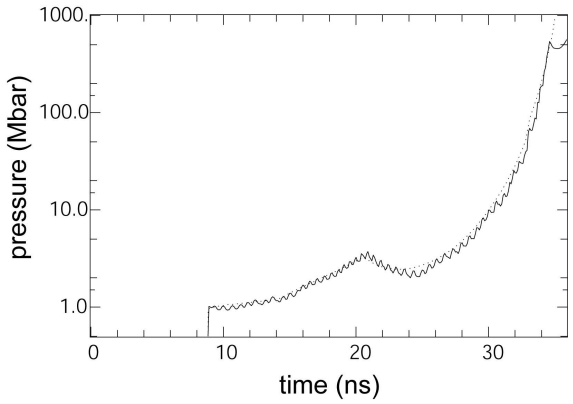


**Figure 7.** Pressure at the fuel-ablator interface as delivered by the target and the laser pulse pictured in figure 6. The dotted line is the desired self-similar pressure history from figure 5.

of the hydrodynamics. A laser wavelength of 351 nm was also used.

Note that the laser pulse intensity rises steeply at the end of the pulse and then drops abruptly to zero. To maintain the self-similar pressure drive, the laser intensity would have had to continue to rise until the very end of the implosion to extremely high values. However, on account of the danger of deleterious laser-plasma instabilities at these intensities, the laser was switched off after crossing an intensity of $2.5 \times 10^{15}\,\mathrm{W/cm^2}$. The resultant flattopping of the pressure, of course, breaks the self-similarity but, as illustrated below, the perturbation introduced by this effect does not unacceptably disrupt the core before the time at which ignition would occur.

The degree to which the pressure delivered by this laser pulse matches that from figure 5 is illustrated in figure 7. The match is clearly quite close up until the point at which the pressure flattops at $\sim 500\,\mathrm{Mbar}$ due to the laser being switched off. The oscillations in the delivered pressure result from the expansion of the discrete simulation zones making up the ablator ("zone popping") as the ablation wave advances through the ablator. These oscillations can be seen to imprint on the density profiles of the the

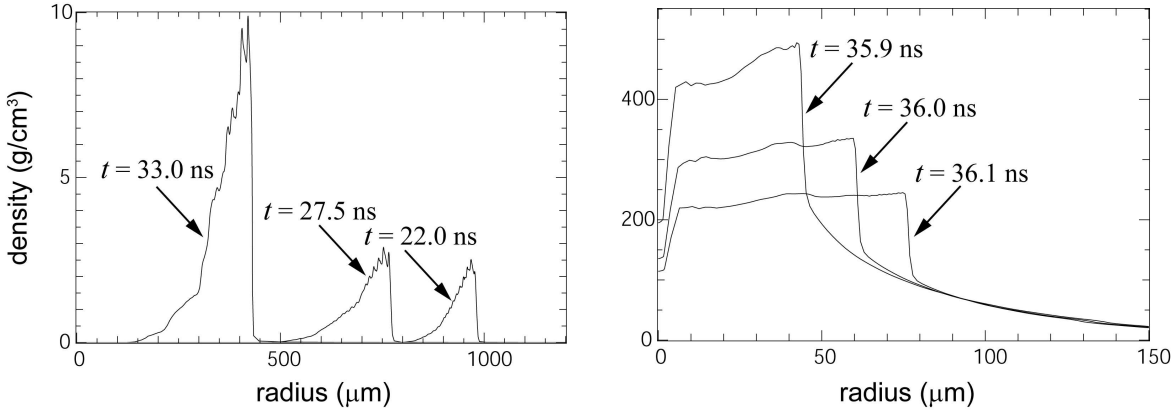


**Figure 8.** Sequential flow profiles shortly before and immediately after the time of void closure for the implosion of the target pictured in figure 6.

shell (in figure 8 below) but do not unacceptably disrupt the implosion. Finer zoning can be used to reduce this effect.

Three selected times from the implosion and stagnation phases for this target are shown in figure 8. Though neither the imploding nor stagnating phases from this simulation are precisely self-similar, the similarities between the exact self-similar results in figure 3 and the non-ideal, laser-driven results in figure 8 are plainly evident. The assembled density in the simulation is in the region of interest for FI ($\sim 300\,\mathrm{g/cm^3}$) [3], and the radial distribution of the density is quite uniform from the center of the implosion to the stagnation shock front. For the times shown in the figure, the fuel areal density ranges from $2.0 - 2.7\,\mathrm{g/cm^2}$. As in the self-similar result, there is virtually no hot spot.

The most notable difference between figure 8 and figures 3 and 4 is evident in the tails of the stagnated density profiles from $r = 100$ to $150\,\mu$m. The density profiles in the laser-driven case are decompressed relative to the ideal case as a consequence of the flattopping of the drive pressure seen in figure 7. Despite this breaking of self-similarity, the density profiles in the core remain quite close between figures 3 and 8.

The total laser energy delivered to this target is a quite reasonable 485 kJ. If successfully ignited, the 0.9 mg fuel mass with an areal density of $2.4\,\mathrm{g/cm^2}$ would give a yield of $\sim 86$ MJ. Assuming an ignition beam energy of 20 kJ, this would give a target gain of $\sim 170$. The peak implosion velocity in this design is $6.0 \times 10^6$ cm/s and represents a peak fuel kinetic energy of 7.0 kJ. Given the 42% coupling efficiency of this target, the hydrodynamic efficiency is then 3.5%. Note that, despite these low hydrodynamic and coupling efficiencies, a quite dense core can yet be assembled at modest laser energy due to the very low in-flight fuel adiabat.

The fuel adiabats from selected times during the implosion and stagnation phases are shown in figure 9. That the flow is highly isentropic, particularly during the implosion phase, as well as on a remarkably low adiabat is apparent. The regions of high entropy to the left and right during the implosion phase correspond to the central

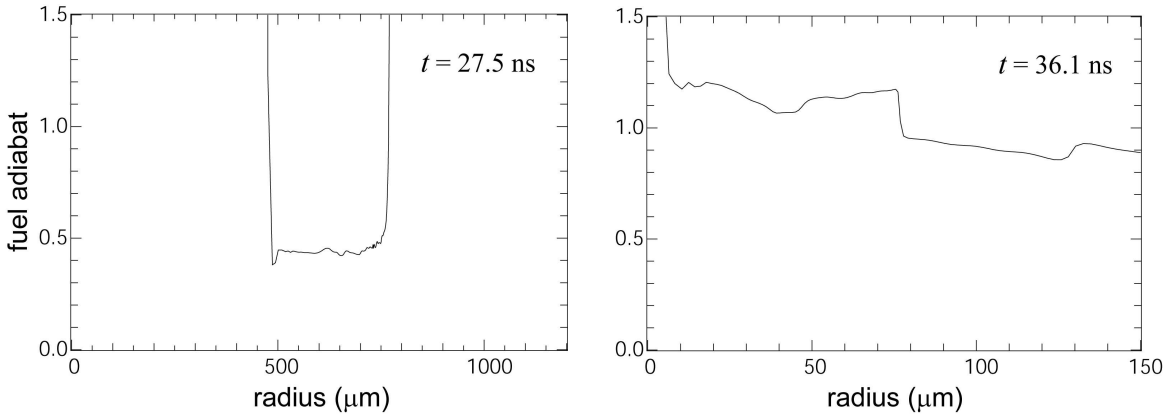


**Figure 9.** Snapshots of the fuel adiabats corresponding to selected times shown in figure 8. The adiabats are defined by $\alpha \doteq p(\text{Mbar})/\left[2.17\rho(\text{g/cm}^3)^{5/3}\right]$.

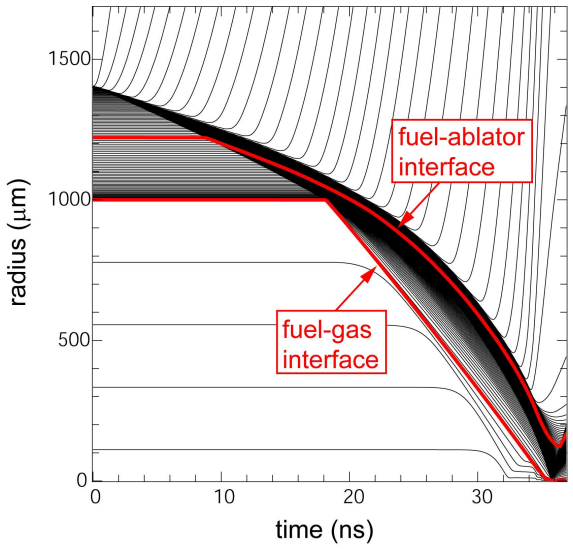


**Figure 10.** Lagrangian trajectories of selected simulation zones from the implosion of the target shown in figure 6. The inner and outer boundaries of the fuel layer are indicated in red.

gas and the ablation regions, respectively. The adiabats are defined relative to the usual Fermi degenerate pressure according to $\alpha \doteq p(\text{Mbar})/\left[2.17\rho(\text{g/cm}^3)^{5/3}\right]$. Note that, for this definition, an adiabat less than unity corresponds to a not fully ionized plasma.

Finally, the Lagrangian trajectories of selected simulation zones from this implosion are shown in figure 10. Also indicated by the red lines are the inner and outer boundaries of the fuel layer. Striking in this plot is the relatively low aspect ratio of the shell ($A \leq 10$) throughout the implosion. Coupled with the near constant velocity of the shell through much of the implosion, *i.e.*, unaccelerated motion, this implosion can be expected to be particularly stable to Rayleigh-Taylor growth and should behave in an essentially 1-D fashion.

## 5. Conclusions

A design has been presented for assembling a quasi-isochoric implosion with nearly zero hot spot volume for FI applications. This design was inspired by the recognition that a particular class of self-similar solutions implodes an initially low-density shell of material into a high-density, quasi-isochoric assembly, as is optimal for FI. Using this idealized self-similar solution as a guide, a direct drive target design was developed including the effects of a realistic equation of state, realistic heat conduction, finite central gas fill, etc. Among other respects, this design is unique in being driven by a single shock followed by a subsequently entirely isentropic compression. Although not perfectly self-similar, the stagnated state of the detailed target design approaches remarkably closely to the self-similar ideal. More importantly, the nearly isochoric implosion assembles the desired density and areal density of $300\,\mathrm{g/cm^3}$ and $2.4\,\mathrm{g/cm^2}$ for the quite modest energy investment of 485 kJ. Of course, the design presented here could easily be scaled to a larger assembled fuel mass and areal density at an increased laser energy. For example, a laser energy of 950 kJ would yield an areal density of $3.0\,\mathrm{g/cm^2}$ with a fuel mass of 1.8 mg.

Several shortcomings remain in the design presented. Foremost, of the 485 kJ delivered to the target pictured in figure 6, only 200 kJ is actually absorbed. A higher absorption fraction would clearly be desirable. This low absorption is a direct consequence of the highest intensity component of the laser pulse occurring very late in the implosion when the target has already significantly shrunk in volume. A large fraction of the laser energy simply misses the target geometrically as a consequence. That the drive pressure, and hence laser intensity, must be high until the very end of the implosion is, however, required in order to maintain as closely as possible the self-similar, isentropic character of the flow. Zooming the laser pulse at the end of the implosion might be employed to improve this absorption.

Similarly, the laser pulse pictured in figure 6 is quite high contrast and of quite high intensity compared with typical direct-drive pulse shapes. This high contrast is a direct consequence of choosing a single shock pulse shape. Choosing a lower aspect ratio target design could reduce this contrast but, as mentioned, incurs the penalty of a less mechanically efficient implosion. Note, however, that this high contrast is stretched over a longer pulse than is typical. Such a high contrast drive would also make problematic realizing these implosions in an indirect-drive configuration.

More broadly, most recent FI target designs feature a cone of dense material to guide the ignition laser pulse to the target center following the hydrodynamic phase of the implosion [30]. This essentially 2-D feature is clearly beyond the scope of the 1-D target considerations discussed here. Integrating the 1-D design given here into a fully 2-D design including a guiding cone would be required.

Nevertheless, it is remarkable that an imploded core as similar to the exact analytical result pictured in figure 3 can be achieved considering the multitude of non-ideal physics processes involved. The applicability of these self-similar solutions

in describing the imploded core configuration in the ICF context has at least been demonstrated. From the perspective of target design, the design presented here opens the possibility of genuinely isochoric implosions for FI.

## Acknowledgments

The authors acknowledge valuable discussions with M. C. Herrmann and A. Kemp. This work was performed under the auspices of the U. S. Department of Energy by the University of California, Lawrence Livermore National Laboratory under Contract No. W-7405-Eng-48.

## References

[1] M. Tabak, J. Hammer, M. E. Glinsky et al. Ignition and high gain with ultrapowerful lasers. *Phys. Plasmas*, 1(5):1626-1634, 1994.

[2] J. D. Lindl. *Inertial Confinement Fusion: the Quest for Ignition and Energy Gain Using Indirect Drive*. American Institute of Physics, New York, 1998.

[3] S. Atzeni. Inertial fusion fast ignitor: Igniting pulse parameter window vs the penetration depth of the heating particles and the density of the precompressed fuel. *Phys. Plasmas*, 6(8):3316-3326, 1999.

[4] M. Tabak, D. Hinkel, S. Atzeni et al. Fast ignition: overview and background. *Fusion Sci. & Technology*, 49:254-277, 2006.

[5] G. I. Taylor. The formation of a blast wave by a very intense explosion I. Theoretical discussion. *Proc. R. Soc. London. Ser. A*, 201:159-174, 1950.

[6] L. I. Sedov. *Similarity and Dimensional Methods in Mechanics*. Academic Press, New York, 1959.

[7] Ya. B. Zel'dovich and Yu. P. Raizer. *Physics of Shock Waves and High-Temperature Hydrodynamic Phenomena*. Academic Press, New York, 1967.

[8] R. Betti and C. Zhou. High-density and high-$\rho R$ fuel assembly for fast-ignition inertial confinement fusion, *Phys. Plasmas*, 12(11):110702, 2005.

[9] R. E. Kidder. Theory of homogeneous isentropic compression and its application to laser fusion. *Nucl. Fusion*, 14:53-60, 1974.

[10] A. Kemp and J. Meyer-ter-Vehn. Stagnation pressure of imploding shells and ignition energy scaling of inertial confinement fusion targets. *Phys. Rev. Lett.*, 86(15):3336-3339, 2001.

[11] S. A. Slutz and M. C. Herrmann. Radiation driven capsules for fast ignition fusion. *Phys. Plasmas*, 10(1):234-240, 2003.

[12] R. B. Stephens, S. P. Hatchett, M. Tabak, C. Steckl, H. Shiraga, S. Fujioka, M. Bonino, A. Nikroo, R. Petrasso, T. C. Sangster, J. Smith, and K. A. Tanaka. Implosion hydrodynamics of fast ignition targets. *Phys. Plasmas*, 12(5):056312, 2005.

[13] C. Ferror Fontan, J. Gratton and R. Gratton. Self-similar spherical implosions. *Phys. Lett. A*, 55(1):35-37, 1975.

[14] G. Guderley. Strong spherical and cylindrical shock fronts near the center of the sphere or the cylinder axis. *Luftfahrtforschung*, 19(9):302-312, 1942.

[15] R. B. Lazarus. Self-similar solutions for converging shocks and collapsing cavities. *SIAM J. Numer. Anal.*, 18(2):316-370, 1981.

[16] K. V. Brushlinskii and Ya. M. Kashdan. On auto-models in the solution of certain problems of gas dynamics. *Amer. Math. Soc. Transl.*, 2(110):1-22, 1963.

[17] J. Meyer-ter-Vehn and C. Schalk. Selfsimilar spherical compression waves in gas dynamics. *Z. Naturforsch*, 37a:955-969, 1982.

[18] Lord Rayleigh. *Scientific Papers*. Cambridge Univ. Press, Cambridge, 1900.

[19] C. Hunter. On the collapse of an empty cavity in water. *J. Fluid Mech.*, 8:241-263, 1960.

[20] G. I. Barenblatt and Ya. B. Zel'dovich. Self-similar solutions as intermediate asymptotics. *Annu. Rev. Fluid. Mech.*, 4:285-312, 1972.

[21] G. I. Barenblatt. *Similarity, Self-similar, and Intermediate Asymptotics.* Consultants Bureau, New York, 1979.

[22] W. Haefele. Zur analytichen behandlung ebener starker instationärer strosswellen. *Z. Naturforsch*, 10:1006-1016, 1955.

[23] W. Haefele. Über die stabilität des strosswellentypus aus der klasse der homologie lösungen. *Z. Naturforsch*, 10:1017-1027, 1955.

[24] R. B. Lazarus. One-dimensional stability of self-similar converging flows. *Phys. Fluids*, 25(7):1146-1155, 1982.

[25] L. P. Thomas, V. Pais, R. Gratton and J. Diez. A numerical study on the transition to self-similar flow in collapsing cavities. *Phys. Fluids*, 29(3):676-679, 1986.

[26] R. Courant and K. O. Friedrichs. *Supersonic Flow and Shock Waves.* Springer, New York, 1948.

[27] M. M. Marinak, G. D. Kerbel, N. A. Gentile, O. Jones, D. Munro, S. Pollaine, T. R. Dittrich, S. W. Haan. Thee-dimensional HYDRA simulations of National Ignition Facility targets. *Phys. Plasmas*, 8(5):2275-2280, 2001.

[28] R. M. More, K. H. Warren, D. A. Young and G. B. Zimmerman. A new quotidian equation of state (QEOS) for hot dense matter. *Phys. Fluids*, 31(10):3059-3078, 1988.

[29] C. Souers Cryogenic properties of heavy hydrogen. Lawrence Livermore National Laboratory Report (unpublished), 1973.

[30] R. B. Stephens, S. P. Hatchett, R. E. Turner, K. A. Tanaka, and R. Kodama. Implosion of indirectly driven reentrant-cone shell target. *Phys. Rev. Lett.*, 91(18):185001, 2003.